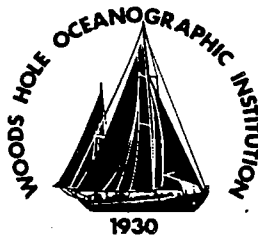


Woods Hole Oceanographic Institution



Biogenic Particle Fluxes at the 34°N 21°W and 48°N 21°W Stations, 1989-1990: Methods and Analytical Data Compilation

by

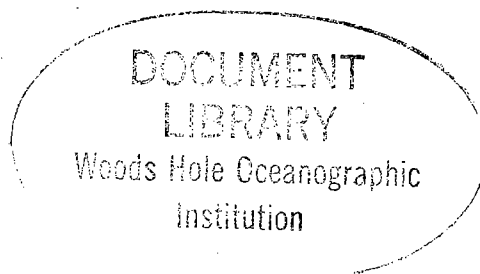
Susumu Honjo and Steven J. Manganini

March 1992

Technical Report

Funding was provided by the National Science Foundation through
Grant No. OCE 88-14228.

Approved for public release; distribution unlimited.



WHOI-92-15

**Biogenic Particle Fluxes
at the 34°N 21°W and 48°N 21°W Stations, 1989-1990:
Methods and Analytical Data Compilation**

by

Susumu Honjo and Steven J. Manganini

Woods Hole Oceanographic Institution
Woods Hole, Massachusetts 02543

DOCUMENT
LIBRARY
Woods Hole Oceanographic
Institution

March 1992

Technical Report



Funding was provided by the National Science Foundation through
Grant No. OCE 88-14228.

Reproduction in whole or in part is permitted for any purpose of the
United States Government. This report should be cited as:
Woods Hole Oceanog. Inst. Tech. Rept., WHOI-92-15.

Approved for publication; distribution unlimited.

Approved for Distribution:

A handwritten signature in black ink, appearing to read 'G. Michael Purdy', is written over a horizontal line.

G. Michael Purdy
Department of Geology & Geophysics

**BIOGENIC PARTICLE FLUXES
AT THE 34°N 21°W AND 48°N 21°W STATIONS, 1989-1990:
METHODS AND ANALYTICAL DATA COMPILATION**

by

Susumu Honjo and Steven J. Manganini
Woods Hole Oceanographic Institution
Woods Hole, MA 02543 USA

March 1992

Data appearing in this Technical Report have been submitted to the United States National Oceanographic Data Center, 1825 Connecticut Avenue, Washington, DC 20235. These data are also available from the United States JGOFS Data Management Office, Woods Hole Oceanographic Institution, Woods Hole, MA 02540.

5 key words: bloom
 North Atlantic Ocean
 ocean interior
 particle flux
 terminal ratio

TABLE OF CONTENTS

Abstract.....	1
Introduction.....	2
Method.....	3
Deployment of Sediment Traps and Mooring Arrays.....	3
Location, depths and timing.....	3
Time-series sediment trap	3
Mooring array.....	4
Laboratory Analysis.....	5
Pre-analysis treatment of samples.....	5
Supernatant analysis.....	5
Water sieving	5
Total dry mass measurement.....	6
Sedimentary component analyses	6
Restoration of dissolved components to particulate flux.....	8
Initial Bottle Water Concentration.....	8
Water Column Concentration.....	8
Final Bottle Water Concentration.....	9
Dissolved Components	9
Total Components.....	9
Formulae	9
Flux Calculations	9
Sample Collecting Time.....	10
Actual Collecting Time.....	10
Normalized Collecting Time	10
Formulae	10
Results.....	11
Annual Particle Flux.....	11
Variability of Particle Fluxes by Period.....	12
Variability of Particle Fluxes by Depth	13

Fluxes of Sedimentary Components	13
Ratios of Critical Biogeochemical Elements	14
Acknowledgments.....	15
References.....	16
Explanation of Figures.....	18
Figures	
Figure 1 Locations.....	20
Figure 2 Transect Profiles.....	21
Figure 3 Mooring Schematics.....	22
Figure 4 Total Mass Fluxes; Annual Variability	23
Figure 5 Component Fluxes; Annual Variability.....	24
Figure 6 Proportions of Component Fluxes; Annual Variability	25
Figure 7 C_{org}/C_{CaCO_3} , Variability in Space and Time.....	26
Figure 8 Ratio Between Biogenic Elements in Episodes	27
Explanation of Tables.....	28
Tables	
<i>Logistics Tables</i>	31
Table 1 Mooring Stations and Trap Depths.....	32
Table 2 Synchronized Open/Close Schedule.....	33
Table 3 Sediment Trap Specifications.....	34
<i>Preparation Tables</i>	35
Table 4 Initial Water: location and depths	36
Table 5 Nutrient Concentration in Initial Water	
Table 5-a at 34°N 21°W.....	37
Table 5-b at 48°N 21°W.....	38
Table 6 "Times" to deliver "Normalized Times".....	39
<i>Summary Tables</i>	40
Table 7 Flux Summary.....	41
Table 8 34°N: Fluxes and Proportions Sedimentary Components.....	42
Table 9 48°N: Fluxes and Proportions Sedimentary Components.....	43

Table 10	34°N: Ratios Between Biogeochemical Elements.....	44
Table 11	48°N: Ratios Between Biogeochemical Elements.....	45
Table 12	"Redfield Ratio"	46
<i>Tables Giving Flux per Period.....</i>		<i>47</i>
Table 13: 34°N		
Table 13-1: 1 km		
Table 13-1-a	Size Fractions.....	48
Table 13-1-b	Fluxes of Ca, C _{inorg} , C _{org} and N _{org}	49
Table 13-1-c	Opal Fluxes.....	50
Table 13-1-d	Phosphorus Fluxes	51
Table 13-1-e	Ratios (Molar) of Critical Elements.....	52
Table 13-2: 2 km		
Table 13-2-a	Size Fractions.....	53
Table 13-2-b	Fluxes of Ca, C _{inorg} , C _{org} and N _{org}	54
Table 13-2-c	Opal Fluxes.....	55
Table 13-2-d	Phosphorus Fluxes	56
Table 13-2-e	Ratios (Molar) of Critical Elements.....	57
Table 13-3: 0.7 km above bottom		
Table 13-3-a	Size Fractions.....	58
Table 13-3-b	Fluxes of Ca, C _{inorg} , C _{org} and N _{org}	59
Table 13-3-c	Opal Fluxes.....	60
Table 13-3-d	Phosphorus Fluxes	61
Table 13-3-e	Ratios (Molar) of Critical Elements.....	62
Table 14: 48°N		
Table 14-1: 1 km		
Table 14-1-a	Size Fractions.....	63
Table 14-1-b	Fluxes of Ca, C _{inorg} , C _{org} and N _{org}	64
Table 14-1-c	Opal Fluxes.....	65
Table 14-1-d	Phosphorus Fluxes	66
Table 14-1-e	Ratios (Molar) of Critical Elements.....	67

Table 14-2: 2 km	
Table 14-2-a	Size Fractions.....68
Table 14-2-b	Fluxes of Ca, C _{inorg} , C _{org} and N _{org}69
Table 14-2-c	Opal Fluxes.....70
Table 14-2-d	Phosphorus Fluxes71
Table 14-2-e	Ratios (Molar) of Critical Elements.....72
Table 14-3: 0.7 km above bottom	
Table 14-3-a	Size Fractions.....73
Table 14-3-b	Fluxes of Ca, C _{inorg} , C _{org} and N _{org}74
Table 14-3-c	Opal Fluxes.....75
Table 14-3-d	Phosphorus Fluxes76
Table 14-3-e	Ratios (Molar) of Critical Elements.....77

**BIOGENIC PARTICLE FLUXES
AT THE 34°N 21°W AND 48°N 21°W STATIONS, 1989-1990:
METHODS AND ANALYTICAL DATA COMPILATION**

by

Susumu Honjo and Steven J. Manganini
Woods Hole Oceanographic Institution
Woods Hole, MA 02543 USA

ABSTRACT

This technical report presents the results of analyses on opal, organic carbon, nitrogen and phosphorus content in each of 156 specimen samples collected from the moored sediment trap experiment that was a part of JGOFS North Atlantic Bloom Experiment. The analyzed samples represent a spatio-temporal matrix formed by 6 time-series sediment traps that provided 26 periods of uniform and synchronized periods of 14 days, except for one longer and one shorter period. Traps were deployed at 3 depths, 1 km, 2 km and 0.7 km above the bottom, and at 2 stations, 34°N 21°W and 48°N 21°W from April 4, 1989 to April 17, 1990, as shown in Tables 1 and 2. There was an 20-day hiatus in September/October 1989 for changeover of the trap moorings. Some samples were unusable because of the intrusion of fish.

Samples were separated into several aliquots by wet-splitting, then water sieved into larger-than- and smaller-than-1-mm sizes. The fluxes of biogeochemical elements and constituents were determined on these aliquots and size fractions for: carbonate by vacuum gasometric method; opal by selective leaching method; reactive phosphorus by high temperature oxidation hydrolysis method; and organic carbon and nitrogen by applying an elementary analyzer. The annual fluxes, fluxes during the bloom, pre- and post-bloom episodes were normalized to a 365-day calendar year (Table 6) and are summarized in Tables 7 to 12. Variability of particle fluxes by each period at the two stations in terms of size fractions, sedimentary constituents and elements are shown in Tables 13 and 14. The molar ratios between pairs of critical biogeochemical elements during each episode and annually, shown at various depths and stations, are included in Tables 10 through 14.

INTRODUCTION

Six automated time-series sediment traps were deployed at three bathypelagic layers along bottom-tethered, moored arrays in the North Atlantic at 34°N 21°W and 48°N 21°W for about a year from the spring of 1989 to the spring of 1990, with the North Atlantic Bloom Study Experiment (NABE) organized by JGOFS and supported by the National Science Foundation, USA. The 34°N station is in the North Atlantic Subtropical Zone while the 48°N station is in the North Atlantic Transition Zone (Bradshaw, 1959; Okada and McIntyre, 1979) representing different physical and biogeographic ocean areas. This trap experiment was characterized by synchronizing the open/close timing of all 6 traps that provided us with a time-space matrix in depth (1, 2 and 4.5 or 5 km) and latitude (1,256 km apart); these conditions were necessary to better understand the rates and processes of exporting biogenic matter from the upper ocean to the interior with regard to detecting oceanographic variabilities in time and space..

The main objective of measuring particle fluxes to the interior of the moderate North Atlantic Ocean at the NABE site by time-series sediment trap array was to understand the magnitude and composition of biogenic particle fluxes throughout a year, in particular during a bloom, and to determine the seasonal variability of mass flux in time and space. Furthermore, we wanted to model the rates and processes of the export of biogenic matter produced in the surface layers to the ocean interior, particularly by comparing changes in the chemistry associated with the 1989 spring bloom to the variabilities in particle fluxes in the ocean interior during the same period.

Our successful field experiment and subsequent laboratory analyses have provided a large body of data that have begun to serve the NABE research community as the basis of many studies (e.g. Altabet *et al.*, 1991; Honjo and Manganini, 1992 and many others in preparation). This report details the analytical results of the biogenic component of fluxes from the experiment with annotation on the analytical methods. We hope this report will be useful as the basis of further investigations of the biogeochemical cycles in the North Atlantic Ocean.

METHOD

Deployment of Sediment Traps and Mooring Arrays

Location, depths and timing.

Two deep ocean mooring arrays were deployed at about 34°N (depth to seafloor: 5,261 m and 5,083 m, for phase 1 and 2) and 48°N (depth to seafloor: 4,418 m and 4,451 m). The approximate locations of sediment trap mooring stations are illustrated in Figure 1. Table 1 gives more detailed information on mooring locations, trap depths and names of ships that were used for deployment and recovery. Three PARFLUX Mark 7G-13 time-series sediment traps with 13 rotary collectors on each were deployed on both moorings for a total of 6 traps. At each of the stations, traps were moored at approximately the same depth relative to the surface and the sea-floor (for the deepest trap); 1 km and 2 km from the surface and 0.7 km above bottom (abbreviated as 0.7 km a.b.) Figure 2 portrays the spatial relationships among the 6 time-series traps.

Arrays were deployed in March and April 1989, recovered and redeployed in September 1989, and totally recovered in April 1990 (Table 1). During the 376-day deployment (including 20 days of hiatus in the middle), each sediment trap was opened and closed 26 times, providing continuous time-series sampling at 14-day intervals, except for two periods. Table 2 lists open/close schedules for which all the traps were uniformly programmed during the experiment. An independent monitoring mechanism installed with each trap (Honjo and Doherty, 1988) confirmed that the entire program was executed correctly and on schedule.

Time-series sediment traps.

Each sediment trap had an aperture of 0.5 m², covered by baffles with 25 mm-diameter cells with the aspect ratio of 2.5. The included cone angle was 42 degrees and the structural frame was built of welded titanium. The opening and closing of all 6 traps was synchronized with an error of less than one minute. The sample containers, 13 for each trap, were filled with *in situ* deep sea water were collected by a 30 liter Niskin bottle prior to the deployment (Table 4). Analytical grade formalin

(S. Wakeham; personal communication, 1988) was added to make a 3% solution buffered with 0.1% sodium borate (Table 4). Each of the 13 sample containers was completely filled with this sea water solution with preservative before the deployment of a trap. Individual sample containers were mechanically sealed from the ambient water before and after each collecting period (Honjo and Doherty, 1988). The specifications of the PARFLUX Mark 7G-13 are presented in Table 3.

Mooring array

The mooring design was based on the PARFLUX Sediment Trap Mooring Dynamics Package that has been used by us since 1979 (Honjo *et al.*, 1992). Figure 3 illustrates the outline of the mooring that was deployed at the 48°N 21°W station during phase 1 as an example. (A detailed design, parts listing and tension calculation of the NABE mooring array is available in Manganini and Krishfield, 1992, Cruise Report). The arrays were designed to maintain an average of 180 kg of vertical tension throughout the tautline, with a total buoyancy of 1,114 kg that was balanced with a 1,590 kg (in-water weight) cast-iron anchor. Sediment traps were attached to a mooring in-line with three 1-m polyethylene-jacketed bridles. The automatic collection mechanism (Honjo and Doherty, 1988) of the 6 sediment traps worked flawlessly throughout the duration of the experiment and provided us with a total of 156 samples each of which represents an individual key to the time-space matrix for the NABE experiment.

Although the recording was not complete, current meters and thermistors that were deployed 1.2 m below the three sediment traps at the 48°N 21°W station (Fig. 3) (Honjo *et al.*, 1989, Cruise Report) recorded no significant turbulence, and currents were generally less than 5 cm sec⁻¹ throughout the year-long deployment. These current meter data were consistent with the reported results of the TOPOGULF Experiment along 48°N (IFREMER, 1987; De Verdiere, 1989). Model calculations obtained from the current record that applied to our mooring at the 34°N and 48°N stations indicated that the traps tilted less than 1° from the vertical during the period of measurement. No significant statistical relationships were found between total flux, particle size groups, particle composition, current direction or strength.

Laboratory Analysis

Pre-analysis treatment of samples

We measured the pH in supernatant in sample containers immediately after recovery of traps (Manganini and Krishfield, 1992, Cruise Report). Sample containers were then refrigerated on board at approximately 2 to 4° C. Particle samples in (original) 250 ml, polyethylene centrifuging sample containers were transported to Woods Hole under refrigeration at approximately 1° to 2° C. We identified no swimmers from all samples collected by our experiment. The impact of swimmers, if any, was relatively small; it appears that they were all included with the >1 mm fractions.

Supernatant analysis

In the shore laboratory, first the liquid in a sample container was decanted and then filtered through a 0.45 µm pore size Nucleopore™ filter leaving approximately 1/3 of the original volume. About 50 ml of filtered liquid was then analyzed for total N, NO₂, NO₃, NH₄, P, PO₄ and SiO₂ using an automatic nutrient analyzer (e.g. Grasshoff *et al.* 1983). We regarded all excess quantities above the ambient concentration as being dissolved from the trapped particles while stored *in situ* before the recovery and added to the particle fluxes after being stochastically converted to solids using the calculation described later (Tables 13 and 14). The remaining liquid in the sampling containers was used as rinse water in the processing of the particulate portion in each specific sample. When additional rinse water was required during the course of analysis, for example, for sample splitting we used filtered and buffered deep Sargasso Sea water containing 3% formalin.

Water sieving

Particle samples were water-sieved through a 1-mm Nitex™ mesh. This was necessary to maintain precision during splitting of the major portion of the sediment that was <1 mm. Common particles in the >1 mm fraction were large aggregates and fragmented gelatinous zooplankton. A sample caught in the 1 mm mesh was then re-suspended in the original seawater, stirred gently and poured onto a grid-printed, 47-mm Nucleopore™ filter with 2-µm pore size, while applying

gentle vacuum suction. While a sample on a filter was wet, the filter with the >1 mm fraction was cut into 4 equal pieces along the printed grid by a Teflon™-coated blade; each aliquot was then immediately put back into the filtered original water for storage. When a >1 mm sample was too small to split, it was dried and homogenized by pulverization.

Sediment that passed through the 1 mm mesh was further water-sieved through a 62 µm Nitex™ sieve. Each fraction was split into 1/4 aliquots and then into 1/40 aliquots by a rotating wet-sediment splitter with 4 and 10 splitting heads (Honjo, 1980). The average error during the splitting of NABE samples into 4 or 10 aliquots was 3.7% for the <1 mm fraction. Wet splitting of the trap-collected sample is justified for multi-disciplinary research including biocoenosis studies. Once particle samples are dried, each becomes inseparable and unidentifiable. Consequently, biocoenosis research such as picking up foraminifera tests or identifying diatom frustules becomes impossible.

Total dry mass measurement

Dry mass was determined by weighing two 1/4 aliquots of >1 mm (whose flux was usually insignificant) and three 1/10 aliquots of <1 mm samples on pre-weighed 47 mm, 0.45 µm Nucleopore filters. Before weighing, the samples were rinsed 3 times with distilled water, dried in an oven at 60° C for 24 hours and cooled in a desiccator for 4 hours. Total flux was calculated from dry weight of the above aliquots divided by aperture area of the trap and the time it was opened.

Sedimentary component analyses

The dried sample was pulverized and homogenized, then the two size fractions were recombined proportionally and analyzed with respect to concentrations of:

- a) Carbonate: as CaCO₃
- b) Biogenic Opal
- c) Organic carbon, nitrogen and hydrogen in the decalcified fraction
- d) Phosphorus

Carbonate content was determined by a method based on a vacuum-gasometric technique developed by Ostermann, *et al.* (1989). A preweighed sample

is introduced into a sealed reaction vessel containing concentrated phosphoric acid. The pressure due to the evolution of CO₂ gas is proportional to the carbonate content when calibrated with appropriate standards and was recorded by a transducer. The results were calculated and reported as carbonate percent in the total sample.

Biogenic opal was estimated from particulate, reactive Si, selectively leaching decalcified samples in a sodium carbonate solution (Eggimann, *et al.*, 1980) and converting the Si content to SiO₂ fluxes. A preweighed sample of approximately 10 mg along with 10 ml of 1 M Na₂CO₃ was sealed in a Teflon™ container. The samples were placed in a shaker bath at 90°C for 3 hours and then filtered through a 47-mm-diameter, 0.45 μm pore size Nucleopore™ filter using an all-plastic filtering apparatus. The filtrate at room temperature was neutralized with 0.2 N HCl using methyl orange as an indicator. After appropriate dilution, content of Si was determined spectrophotometrically (Strickland and Parsons, 1972). The Si content was then converted to SiO₂ and reported as particulate opal flux.

Reactive (biogenic) phosphorus content was determined by the Solorzano and Sharp method that was based on the dissolution of phosphorus by an acid after ashing, using MgSO₄ as an oxidant. A preweighed sample was placed into a glass centrifuge tube along with 2 ml of 0.017 M MgSO₄ and was dried at 90°C. The centrifuge tube containing the sample was ashed at 500°C for 2 hours. After cooling, 5 ml of 0.2 M HCl was added and, with the centrifuge tube capped, was heated at 80°C for 30 min. At room temperature, 5 ml of distilled H₂O with one ml of reagent (Strickland and Parsons, 1972) was added and the centrifuge tube was shaken in a vortex shaker, then centrifuged. The concentration of phosphorus was determined spectrophotometrically in the supernatant and the results were reported as particulate opal flux.

Preweighed samples on precombusted glass fiber filters were decalcified using 1N phosphoric acid. Organic carbon, nitrogen and hydrogen were analyzed using a Perkin-Elmer Elemental Analyzer Model 240C on the decalcified samples.

Using the method that was applied in this paper, the lithogenic particles were too small to detect and were usually within the analytical error.

Restoration of dissolved components to particulate flux

The dissolution of collected particles in a bottle may occur as soon as particles arrive in the bottle while it is open, or later when it is sealed. Assuming that all dissolved portions remained in the recovered bottle, we restored the dissolved components of Si, P and N by analyzing the supernatants in sample bottles. We assumed that the elevated concentration above the sea water initially used to fill the bottles was caused by dissolved components. During the deployment of a trap, the sample bottles were open to the water column only for the duration of collecting periods. While a bottle was open, the bottle water which was placed in the bottle before deployment is exchanged with ambient water. In case the nutrient concentration of the initial bottle water is not equal to that of the ambient water, a correction had to be made; we assumed that one half of the initial water was diluted by the ambient water while the bottle was open (Tables 4, 5-a and 5-b). In practice, the effect on calculating particle flux by the difference of nutrients in the initial sea water was within analytical error.

Si and P concentrations in the final bottle water are at least twice the water column concentration and in most cases an order of magnitude higher, as indicated in Tables 5-a and 5-b. NO_3 concentration in the bottle water was about equal to or less than the concentration in the initial bottle water (Tables 5-a and 5-b). We report total N without correction by adding the dissolved component.

We define the terms and formula for dissolved component fluxes as follows:

Initial Bottle Water Concentration

The concentration of nutrients in water that was put into a sample bottle before deployment.

Water Column Concentration

The concentration of nutrients in $\mu\text{g-at kg}^{-1}$ in the water column at each station at each depth of each trap (Table 4). We applied following data set: Honjo *et al.*, 1989 (Cruise Report); De Baar, 1990 (Data Report); Slagle and Heimerdinger 1991 (Data Report)

Final Bottle Water Concentration

The concentration of nutrients in the liquid portion of a sample bottle after recovery. Same as "dissolved" in Tables 13 and 14.

Dissolved Components

We assumed the excess level above ambient water column nutrients concentration were added by dissolution of particles.

Total Components

Sum of particulate and dissolved components (Tables 13 and 14).

Formulae

1. Weight of Dissolved Component = (Final Bottle Concentration) -
(Water Column Concentration) $\times \frac{250 \text{ ml}}{1000\text{ml}}$ \times atomic mass
2. Dissolved Component Flux = $\frac{\text{Weight Dissolved Component}}{\text{time} \times \text{aperture area (0.5 m}^2\text{)}}$
3. Percent Flux =

$$\frac{\text{Dissolved Component Flux}}{(\text{Dissolved Component Flux}) + (\text{Particulate Component Flux})} \times 100$$

Flux Calculations

We describe particle flux in four timescales in this report: annually, per episode (pre-bloom, bloom and post-bloom; Honjo and Manganini, 1992), per period and daily. Flux per period was obtained by direct measurement during one 14-day open trap period (except for one longer and one shorter period, Table 2). All periods started/ended at 12:00 GST. The annual flux is the flux of particles during 365 days, including all three episodes; pre-bloom, bloom and post-bloom. Each episode was characterized by the quantity of particle fluxes (Honjo and Manganini, 1992) (Fig. 4).

Although the rotating mechanism of the sediment traps worked flawlessly, there were periods where the samples were found to be unusable, or were absent, due to the intrusion of Argentine fish (*Argentina sphyraena*) into the sample bottles, blocking the mouth of the sample bottles, or due to accidental loss of 2 samples during transportation (Fig. 4). Also the NABE trap experiment was interrupted for 20 days in September 1989 for change-over of moorings. Therefore it was necessary to estimate fluxes per episode and per calendar year using averaging methods described below. Annual and episodic fluxes in Tables 7 through 11 were based on this normalized collecting time. Table 6 shows total days and the percentages of sample collection time, actual collecting time and normalized collecting time. Definitions used were:

Sample Collecting Time

The duration of time that samples were collected; does not include hiatus or fish-blocked samples. Total time was different for each trap.

Actual Collecting Time (in days)

The duration of time for the entire collection schedule including hiatus and blocked samples. Total of 378 days for all traps.

Normalized Collecting Time (in days)

Elapsed time as normalized to one year, 365 days.

Formulae

1. Average Flux ($\text{mg m}^{-2} \text{ day}^{-1}$) =

$$\frac{\text{total weight (mg)} \times \text{aperture of trap (0.5 m}^2\text{)}}{\text{sample collecting time}}$$

2. Percent Actual Collection Time (%) = $\frac{\text{actual elapsed time}}{378 \text{ days}} \times 100$

$$3. \text{ Normalized Elapsed Time (days)} = \frac{\text{Percent Actual Collection Time} \times 365}{100}$$

$$4. \text{ Normalized Period Flux (g m}^{-2} \text{ period}^{-1}) = \frac{(\text{Average Flux mg m}^{-2} \text{ day}^{-1}) \times (\text{Normalized Elapsed Time})}{100}$$

$$5. \text{ Total normalized yearly flux} = (\text{Normalized Pre-bloom Flux}) + (\text{Normalized Bloom Flux}) + (\text{Normalized Post-bloom Flux})$$

$$6. \text{ Normalized Percent Yearly Flux Per Period} =$$

$$\frac{\text{Normalized Period Flux}}{\text{Total Yearly Flux (g m}^{-2} \text{ yr}^{-1})} \times 100$$

RESULTS

Annual Particle Flux

Table 7 summarizes total annual particle fluxes and particle fluxes during pre-, post- and bloom episodes. Table 8 (34°N station) and Table 9 (48°N station) show fluxes of critical sedimentological and biogeochemical components during each episode and their proportions in the annual fluxes.

Annual mass flux normalized to 365 days at the 34°N station, 2 km and 0.7 km a.b. was 22.4 and 21.2 g m⁻² yr⁻¹ respectively. At the 48°N station the total flux from equivalent levels was 26.9 and 26.2 g m⁻² yr⁻¹, respectively (Table 7). These were compared with a 6-year mean annual flux measured near Bermuda (32°N 64°W); which was 16.3 g m⁻² yr⁻¹ (1 km a.b.) (Deuser, 1986). Annual fluxes measured from 1983 to 1986 in the Nordic Seas ranged from 28.4 (76°N 11°E) to 7.2 g m⁻² yr⁻¹ (78°N 01°E) (Honjo, 1990).

Total annual fluxes at the 1-km depth at the 34°N and 48°N stations were 19.4 and 19.9 g m⁻² yr⁻¹ respectively and were smaller than the annual mass fluxes measured at the two deepest traps. At the 34° station this was attributed to the intrusion of a fish during JD 119 period (mid-date, April 29, 1989) that accidentally plugged the lower end of the trap (Fig. 4). As shown in Table 8 (34°N 21°W station) and Table 9 (48°N 21°W station), as well as in Figure 6, calcium carbonate (CaCO₃) was the largest component of settling particles. Particulate organic matter (POM) determined by combustion loss and biogenic opal followed. At 2 km deep, the concentrations of CaCO₃, POM and opal were 61.8, 28.8 and 9.1% at the 34°N station and 55.3, 23.0 and 21.9% at the 48°N station, respectively. At 0.7 km a.b., the concentrations of CaCO₂, POM and opal were 60.8, 29.6 and 9.4% at the 34°N station and 58.8, 19.9 and 21.4% at the 48°N station, respectively.

Variability of Particle Fluxes by Period

Tables 13 (34°N) and 14 (48°N) show the seasonal evolution of total particle fluxes, fluxes of particles in two sizes and basic sedimentational and biogeochemical constituents per period. Particle fluxes during each period are plotted with time in Figures 4 and 5. The proportions of constituents in total flux is illustrated in Figure 6. An episode of high particle flux (particle bloom) was observed during springtime at both stations (Fig. 4).

We defined a particle bloom episode as a rapid and continuous increase in particle flux to a peak or peaks, followed by a rapid and consistent decrease to the background flux (Honjo and Manganini, 1992). The boundaries of each episode were first defined at 1 km; then these boundaries were shifted to one period later for the 2-km depth; and then again to one more period later for the 0.7-a.b. depth. At both stations and at all depths no complete spring bloom was observed during this experiment; when the first set of sediment traps was deployed the 1989 spring bloom was already in process; the 1990 bloom was still continuing when the second-phase traps were recovered. We combine years 1989 and 1990 to show one complete bloom cycle as illustrated in Figure 4.

At both stations, a spring particle bloom consisted of two or three outstanding peaks separated by about one month (Figs. 4 and 5). There was a relatively long duration between the two blooms, when the particle fluxes were far smaller and

more stable with time. These periods can be divided into pre- and post-particle-bloom episodes. Distinction of the three episodes involved subjective judgment.

Variability of Particle Fluxes by Depth

The succession of flux variability which is seen in a graph where all periods are plotted with time at shallower depths, was imprinted at deeper levels with or without time-lags. As illustrated in Figures 4 and 5, by comparing the "peak-valley" succession within the 1990 spring bloom at the 34°N station in 1990, for example, the penetration of total flux from 1,248 m to 1,894 m was shifted for one sampling period (14 days). On the other hand, also as illustrated in Figure 4, the peak-valley pattern of fluxes and components during the spring bloom observed at 1,894 m in the spring of 1990 at the 34°N station was repeated at 4,391 m without apparent delay within the 14 days of sampling resolution. At the 48°N station in spring 1989, the later portion of the bloom at 1 km was not as elaborately represented as at the two deeper traps. Peak fluxes found during the bloom at the 2-km trap were fused into a single broader peak at 3,718 m deep. The relatively short arrival time of particles to subsequently deeper traps suggested a rapid and nondiscriminatory settling of particles at both stations.

There was a third but less outstanding peak of particle flux at the end of the post-bloom period at the 48°N 21°W station in JD 262 period (September 19, 1989). This small peak, characterized by relatively enriched organic matter, was repeated at all depths, arriving without delay at the deeper traps. No such similar peak was observed at the 34°N station during its post-bloom period (Fig. 4).

Fluxes of Sedimentary Components

The average fluxes of sedimentary components and their percentage in the total annual flux in each episode: CaCO₃, opal, particulate organic carbon, nitrogen and particulate reactive phosphorus are given in Tables 8 and 9. Tables 13 and 14 show the fluxes of CaCO₃, particulate organic carbon, nitrogen (in "b-series" tables), SiO₂ as opal (in "c-series" tables) and particulate phosphorus (in "d-series" tables). The proportion of dissolved SiO₂ and P with particulated SiO₂ and P are shown in Tables 13 and 14, in percent or ppm by dry weight (in "c-series" and "d-series" tables).

Ratios of Critical Biogeochemical Elements

The molar ratios between a several pairs of critical biogeochemical elements during each period and depths were calculated as illustrated in the "e-series" of Tables 13 and 14.

Ca (in biogenic calcite and aragonite)	<i>vs.</i>	Si (in opal)
C (total organic)	<i>vs.</i>	N (organic)
C (total organic)	<i>vs.</i>	P (total reactive)
N (organic)	<i>vs.</i>	P (total reactive)
C (total organic)	<i>vs.</i>	Si (in opal)

In particle fluxes, the terminal ratio is a constant ratio of fluxes of two chemical species, which is attained as particles settle through the water column. Terminal ratios were observed in specific combinations of elemental fluxes. As two particulate chemical compounds settle, the ratio of their molar fluxes changes as depth increases, but generally reaches a constant ratio at a depth which may vary from area to area. The terminal ratio, however, does not vary with season, but may differ geographically.

As an example, variability of ratios between organic carbon (C_{org}) *vs.* carbon in $CaCO_3$ (C_{inorg}) at the 48°N station at each depth and period, are illustrated in Figure 7. C_{org}/C_{inorg} ratios varied substantially in the shallow levels, but reached more consistency at 4,418 and 4,451 m. The C_{org} *vs.* C_{CaCO_3} ratio per each period became 0.57 and 0.54 at 0.7 km a.b. at the 34°N and 48°N stations, respectively, with a small standard deviation from the mean (Fig. 7). Other examples are that the terminal ratios of Ca and Si at the 34°N and 48°N stations were 4 and 2, respectively, and the terminal ratio of C and P at the 34°N station was 150 (Fig. 8).

Changes of critical biogeochemical ratios by episode are illustrated in Figure 8. The C/P ratio, for example, reached the terminal ratio at 150 at 0.7 km a.b. The C : N : P molar ratio at the deepest trap was 154 : 18 : 1 at 34°N station and 148 : 18 : 1 at the 48°N station (Table 12).

ACKNOWLEDGMENTS

We are grateful to the Joint Global Ocean Flux Program for providing the opportunity to conduct this experiment. We thank Richard Krishfield for assisting in all NABE mooring deployment and recovery cruises. Kenneth Doherty contributed to the success of the program through continuously improving the reliability of the time-series sediment traps. The professionalism of the officers and crew of R/V Atlantis II, R/V Endeavor and HMS Charles Darwin made this difficult deployment of complex mooring arrays, often in high seas at mid-night, sometimes in snowstorms, successful, resulting in all instruments being recovered without incidents. McLane Research Laboratories, Inc. provided all spare parts for the Mk 7G-13 sediment traps and moorings without charge. Katherine Brown expertly laid out the tables in the Technical Report. This program was supported by National Science Foundation under Grant Number OCE 88-14228 (JGOFS/NABE program).

REFERENCES

- Altabet, M. A., Deuser, W. G., Honjo, S., and Stienen, C., 1991. Seasonal and depth-related changes in the source of sinking particles in the North Atlantic, *Nature*, **345**: 136-139.
- Bradshaw, J. S., 1959. Ecology of living planktonic foraminifera of the North and Equatorial Pacific ocean. *Cushman Found. Foram. Res., Contr.* **10**(2), 25-64.
- De Baar, W. J. W., 1990. *Data Report; Joint Global Ocean Flux Study, First Report: R. V. Tyro, Leg 1, Den Helder – Reykjavik – Funchal, 31 July to 11 September 1989*. SOZ Data Report 1990, Nederlands Instituut Voor Onderzoek der Zee. 138 pp.
- Deuser, W. B., 1986. Seasonal and interannual variations in deep-water particle fluxes in the Sargasso Sea and their relation to surface hydrography, *Deep-Sea Research*, **33**: 225-246.
- De Verdiere, C., 1989. Mesoscale variability transition from the Western to the Eastern Atlantic along 48 degree N, *J. Phys. Oceanogr.* , **19**(8): 1149-1170.
- Eggimann, D. W., Manheim, F. T., and Betzer, P. R., 1980. Dissolution and analysis of amorphous silica in marine sediments. *Jour. Sediment Petrol.* **50**: 215-225.
- Grasshoff, K., Ehrhardt, M, and Kremling, K., (eds.), 1983. *Method of Sea-Water Analysis*. Weinheim, Verlag Chemie, 419 pp.
- Honjo, S., 1980. Material fluxes and modes of sedimentation in the mesopelagic and bathypelagic zones, *Journal of Marine Research*, **38**: 53-97.
- Honjo, S., 1990. Particle Fluxes and Modern Sedimentation in the Polar Oceans, Chapter 12 in Smith, W. O., Jr., (ed.), *Polar Oceanography*, Academic Press, New York, Vol. II, p. 322-353.
- Honjo, S. and Doherty, K. W., 1988. Large aperture time-series sediment traps; design objectives, construction and application. *Deep-Sea Research*, **35**(1): 133-149.
- Honjo, S. and Manganini, S. J., 1992. Annual Biogenic Particle Fluxes to the Interior of the North Atlantic Ocean; Studies at 34°N 21°W and 48°N 21°W. *Deep-Sea Research* (accepted).

